

Sub-100 fs mid-infrared pulses as driver for a table-top hard x-ray source

Jannick Weisshaupt, Vincent Juvé, Shian Ku, Marcel Holtz, Michael Woerner and Thomas Elsaesser

Max-Born-Institut für Nichtlineare Optik und Kurzzeitspektroskopie, 12489 Berlin, Germany
juve@mbi-berlin.de, woerner@mbi-berlin.de

Skirmantas Ališauskas, Audrius Pugžlys and Andrius Baltuška

Photonics Institute, Vienna University of Technology, Gusshausstrasse 27-387, A-1040 Vienna, Austria
baltuska@tuwien.ac.at

Abstract: Midinfrared powerful 90 fs pulses at a wavelength of $\lambda = 3.9 \mu\text{m}$ drive a femtosecond hard x-ray source (Cu $K\alpha$: $\hbar\omega = 8.05 \text{ keV}$). Up to 10^8 X-ray photons/pulse are generated which is twice as many as with 800 nm drivers of a 100 times higher peak intensity.

© 2014 Optical Society of America
OCIS codes: 140.7240, 140.7090

Ultrashort hard x-ray pulses are sensitive probes of structural dynamics on the picometer length and femtosecond time scales of electronic and atomic motions [1, 2]. Recent progress in generating such pulses has initiated new directions of condensed matter research [3, 4]. When applying laser-driven x-ray sources in such studies, the signal-to-noise ratio is eventually determined by the shot noise in detecting x-ray photons. Thus, new concepts for generating a higher hard x-ray flux are requested and of high current interest. Here, we present the first table-top femtosecond hard x-ray source driven by intense mid-infrared pulses ($\lambda = 3.9 \mu\text{m}$).

Table-top femtosecond x-ray sources are based on the interaction between an intense optical field and a metallic target. The key steps for producing hard x-ray photons are depicted by Fig. 1a: (1) field-induced extraction of electrons from the metal target, (2) electron acceleration in vacuum by the very strong laser field and (3) electron re-entrance into the target, which leads to x-ray generation via collisional inner-shell ionization followed by a radiative transition of an outer-shell electron into the unoccupied inner shell. For laser intensities above a few 10^{15} W/cm^2 , the tunneling barrier is nearly suppressed and electrons close to the Fermi level are extracted with a probability close to one [5]. The two key parameters influencing the generated x-ray flux are the wavelength λ and intensity I of the optical driver. The maximum kinetic energy gained by the electrons during the acceleration process is proportional to $I\lambda^2$. One expects that the electron acceleration efficiency is much better at longer wavelengths since the optical period is longer.

In our experiments we use powerful mid-infrared pulses generated in an Optical Parametric Chirped Pulse Amplification (OPCPA) scheme [6] which delivers up to $W = 6 \text{ mJ}$ per pulse (pulse duration $\Delta t = 90 \text{ fs}$) at a wavelength of $\lambda = 3.9 \mu\text{m}$ and a repetition rate of 20 Hz. The p-polarized light was steered into a vacuum chamber and focused down to a diameter of $d_{\text{FWHM}} = 21 \mu\text{m}$ onto the copper target (thickness of $20 \mu\text{m}$) under an angle of incidence of $\theta = 41^\circ$. Of the entire x-ray flux emitted in a solid angle of 4π , a small part corresponding to $2.4 \times 10^{-8} \text{ sr}$, is detected in a transmission geometry using a calibrated energy-resolving CdTe detector. The typical spectrum ($W = 5.2 \text{ mJ}$, Fig. 1b) consists of the characteristic line emission of Cu $\hbar\omega_{K\alpha} \simeq 8.0 \text{ keV}$ and $\hbar\omega_{K\beta} \simeq 8.9 \text{ keV}$ and the Bremsstrahlung radiation which extends up to 70 keV.

In Fig. 1c, we plot the $K\alpha$ photons per shot emitted into the full solid angle 4π (red circles: $\lambda = 3.9 \mu\text{m}$) as a function of the driver intensity. For comparison we show results measured with a $\lambda = 800 \text{ nm}$ driver (blue circles) [7, 8]. The $\lambda = 3.9 \mu\text{m}$ data show a steep increase of the $K\alpha$ flux of about 3 orders of magnitude (maximum: $8 \times 10^7 \text{ K}\alpha$ photons per shot) when increasing the intensity on the target from $I = 10^{15}$ to 10^{16} W/cm^2 . For the $\lambda = 800 \text{ nm}$ driver we observe a maximum of $4 \times 10^7 \text{ K}\alpha$ photons per shot and a similar increase for the intensity range from $I = 10^{17}$ to 10^{18} W/cm^2 , i.e., for 100 times higher intensities. The experimental data (symbols in Fig. 1c) are in excellent quantitative agreement with theoretical calculations based on the three steps model described above (solid lines in Fig. 1c). Our model predicts a further increase of $K\alpha$ -flux with intensity for the $\lambda = 3.9 \mu\text{m}$ driver whereas the $\lambda = 800 \text{ nm}$ drivers are close to their saturation limits. Thus, the experiments presented here demonstrate the expected $I\lambda^2$ scaling for laser-driven hard x-ray sources paving the way for future table-top systems with up to $10^{13} \text{ K}\alpha$ photons per second using mid-infrared drivers in the kHz regime.

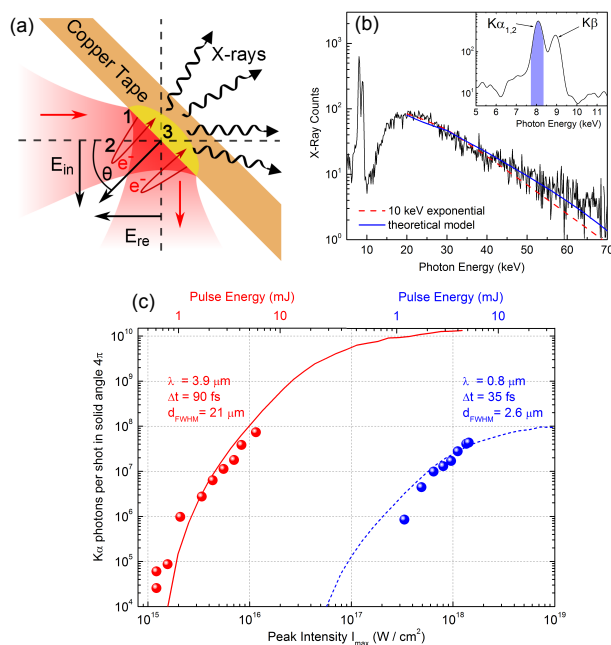


Fig. 1. (a) Schematic of the laser-target interaction geometry and the x-ray generation process. (b) Measured x-ray spectrum using the $\lambda = 3.9\mu\text{m}$ driver. The two peaks are the Cu characteristic lines $K\alpha_{1,2} \simeq 8.0\text{ keV}$ and $K\beta = 8.9\text{ keV}$. The dashed line is an exponential fit to the Bremsstrahlung with a photon temperature of 10 keV. Inset: Characteristic x-ray emission lines. The blue-shaded area denotes the energy interval over which the $K\alpha$ flux is integrated in the intensity dependent data. (c) Comparison of experiment (symbols) with theory (solid and dashed lines) for a $20\mu\text{m}$ thick Cu band illuminated under $\theta = 41^\circ$ angle of incidence. Plotted is the number of $K\alpha$ photons per shot emitted in the solid angle 4π as a function of the peak intensity for the mid-infrared (red symbols) and 800 nm pulses [7, 8] (blue symbols). Solid lines in (b) and (c) are results of model calculations.

References

1. C. Bostedt et al., *Ultra-fast and ultra-intense x-ray sciences: first results from the Linac Coherent Light Source free-electron laser*, Journal of Physics B **46**, 164003 (2013).
2. T. Elsaesser, M. Woerner *Perspective: Structural dynamics in condensed matter mapped by femtosecond x-ray diffraction*, Journal of Chemical Physics **140**, 020901 (2014)
3. B. Freyer, F. Zamponi, V. Juvé, J. Stingl, M. Woerner, T. Elsaesser and M. Chergui, *Ultrafast inter-ionic charge transfer of transition-metal complexes mapped by femtosecond X-ray powder diffraction*, The Journal of Chemical Physics **138**, 14 (2013)
4. V. Juvé, M. Holtz, F. Zamponi, M. Woerner, T. Elsaesser, and A. Borgschulte, *Field-driven dynamics of correlated electrons in LiH and NaBH₄ revealed by femtosecond x-ray diffraction*, Phys. Rev. Lett. **111**, 217401 (2013)
5. S. V. Yalunin, M. Gulde, C. Ropers, *Strong-field photoemission from surfaces: Theoretical approaches*, Phys. Rev. B **84**, 195426 (2011)
6. G. Andriukaitis, T. Balčiūnas, S. Ališauskas, A. Pugžlys, A. Baltuška, T. Popmintchev, M. Chen, M. Murnane and H. Kapteyn, *90 GW peak power few-cycle mid-infrared pulses from an optical parametric amplifier*, Opt. Lett. **36**, 2755–2757 (2011)
7. N. Zhavoronkov, Y. Gritsai, M. Bargheer, M. Woerner, T. Elsaesser, F. Zamponi, I. Uschmann and E. Förster, *Microfocus CuK α source for femtosecond x-ray science*, Opt. Lett. **30**, 1737–1739 (2005)
8. F. Zamponi, Z. Ansari, C.v.K. Schmising, P. Rothhardt, N. Zhavoronkov, M. Woerner, T. Elsaesser, M. Bargheer, T. Trobitzsch-Ryll and M. Haschke, *Femtosecond hard x-ray plasma sources with a kilohertz repetition rate*, Appl. Phys. A **96**, 51–58 (2009)